Gramicidin Channel Kinetics under Tension

M. Goulian,* O. N. Mesquita,*# D. K. Fygenson,* C. Nielsen,§ O. S. Andersen,§ and A. Libchaber*#
*Center for Studies in Physics and Biology, Rockefeller University, New York, New York 10021; #NEC Research Institute, Princeton, New Jersey 08540; and §Department of Physiology and Biophysics, Cornell University Medical College, New York, New York 10021 USA

ABSTRACT We have measured the effect of tension on dimerization kinetics of the channel-forming peptide gramicidin A. By aspirating large unilamellar vesicles into a micropipette electrode, we are able to simultaneously monitor membrane tension and electrical activity. We find that the dimer formation rate increases by a factor of 5 as tension ranges from 0 to 4 dyn/cm. The dimer lifetime also increases with tension. This behavior is well described by a phenomenological model of membrane elasticity in which tension modulates the mismatch in thickness between the gramicidin dimer and membrane.

INTRODUCTION

The local lipid environment plays an important role in determining membrane-protein structure and function (Devaux and Seigneuret, 1985; Bienvenüe and Marie, 1994). However, the relative roles of nonspecific membrane-protein interactions, mediated by bilayer elasticity, versus specific interactions, which depend on the detailed chemistry of the lipids and proteins, have not been elucidated. A variety of theories of nonspecific interactions have been proposed, but there has been relatively little in the way of quantitative measurements to test and refine these models (for reviews see Sackmann, 1983; Abney and Owicki, 1985; Gennis, 1989; Mouritsen and Bloom, 1993; Goulian, 1996).

In this paper we describe the effect of membrane tension on the kinetics of gramicidin A, a channel-forming peptide that can serve as a local probe of bilayer elasticity (Elliott et al., 1983; Sawyer et al., 1989; O'Connell et al., 1990; for reviews see Andersen et al., 1996; Koeppe and Andersen, 1996). Gramicidin A is a 15-amino acid hydrophobic peptide that forms cation-selective channels by the transmembrane association of two nonconducting monomers (Bamberg and Läuger, 1973; Veatch et al., 1975; O'Connell et al., 1990; Cifu et al., 1992) (Fig. 1). Single-channel recording therefore provides a convenient means of monitoring the state of the peptide (i.e., dimer versus monomers). The kinetics of dimer formation and dissociation depends on the interaction between the dimer and membrane. Varying membrane tension modulates the strength of this interaction.

It is often difficult to interpret experiments that probe membrane elasticity at the small length scales relevant to protein structure and function because of the presence of multiple components in the bilayer. Biological membranes are composed of hundreds of different lipids and proteins, and model membrane systems suitable for electrophysiological studies of function often contain varying amounts of hydrocarbons such as decane or squalene, and occasionally charged lipids or cholesterol, to improve membrane stability and adhesive properties. In these systems one needs to consider the local membrane composition, which couples to membrane elasticity. This is an interesting question, which is likely to be important in vivo. However, without concomitant measurements of the local composition, it becomes difficult to interpret the data quantitatively.

We avoid this problem of multiple membrane components by combining pipette aspiration (Kwok and Evans, 1981) and single-channel recording techniques to control membrane tension, while measuring channel kinetics in bilayer vesicles composed of only a single lipid, dioleoylphosphatidylcholine (DOPC). We find that the dimer formation rate exhibits a remarkably strong tension dependence, increasing by a factor of 5 as tension ranges from ~0 to 4 dyn/cm. The dimer lifetime also increases with tension, but to a lesser extent. We argue that for gramicidin the essential effect of tension is to thin the membrane. Our results are well described by a phenomenological model of bilayer elasticity (Huang, 1986), in which tension changes the thickness mismatch between gramicidin and the bilayer.

MATERIALS AND METHODS

Vesicle preparation

The preparation of vesicles followed a modification of the procedures described by Reeves and Dowben (1969) and Needham and Evans (1988). Purified [Val^1]gramicidin A (VgA) and [Gly^1]gramicidin A (GgA) were a gift from R. E. Koeppe, II. DOPC dissolved in ethanol (100 mg/ml) (Avanti Polar Lipids, Birmingham, AL) was mixed with a solution of gramicidin dissolved in ethanol (total volume 20–50 μl), deposited on a clean roughened teflon square (~1 cm × 1 cm) in a glass vial, and dried overnight under house vacuum at room temperature. Molar ratios of gramicidin to DOPC were in the range 0.3–1.0 × 10^{-7} and 0.6–1.2 × 10^{-6} for VgA and GgA, respectively. The vial containing the dried gramicidin-DOPC deposit was loosely capped and placed in a closed plastic box with an excess of water to provide a water-saturated atmosphere and incubated at 47°C for 1 h. A solution consisting of 0.5 M sucrose,

Received for publication 17 July 1997 and in final form 14 October 1997.

Address reprint requests to Dr. Mark Goulian, Center for Studies in Physics and Biology, Rockefeller University, 1230 York Ave., New York, NY 10021. Tel.: 212-327-8183; Fax: 212-327-8544; E-mail: goulian@menard.rockefeller.edu.

Dr. Mesquita is on sabbatical leave from Universidade Federal de Minas Gerais, Belo Horizonte, MG, Brazil.

Dr. Fygenson's present address is Department of Molecular Biology, University of Southern California, Los Angeles, CA 90089.

0006-3495/98/01/328/10 $2.00

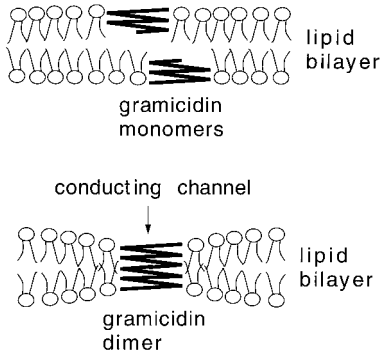

FIGURE 1 Sketch of the gramicidin monomer and dimer states in a lipid bilayer. The dimer forms a conducting channel. Because the thickness of the dimer is less than the thickness of the bilayer, the dimer compresses the membrane.

acidified to pH 2.6 with HCl (1 ml), was then gently added, the cap was tightened, and the sample was further incubated at 47°C for 8 h in the box. A dense dispersion of vesicles was harvested from the cloudy fraction floating near the surface of the sucrose solution (~100 μl).

With time, DOPC will be hydrolyzed at the low pH (pH 1) at which our measurements were made (see below). We examined the extent of this problem by incubating DOPC suspensions with either 0.1 or 1 M HCl for both 1 and 3 h at room temperature (25–30°C) and examining the reaction mixture by thin-layer chromatography on silica plates (Whatman LK6D; Whatman, Clifton, NJ), using a mobile phase consisting of chloroform: methanol:water (65:45:4 v/v). The detection limit was 10% hydrolysis, determined with serial dilutions of lysophosphatidylcholine. There was no detectable hydrolysis after 3 h of incubation in either 0.1 or 1 M HCl. (The lipids were completely hydrolyzed after 60 h of incubation at room temperature in either 0.1 or 1 M HCl.)

Pipette aspiration and electrical recording

Pipette aspiration and video microscopy were performed on a modified version of the apparatus described by Elbaum et al. (1996) and Fygenson et al. (1997) (Fig. 2 *A*). The sample cell consisted of an o-ring (1/8 inch × 7/8 inch) sealed to a 0.17-mm coverslip with paraffin. The cell was mounted on a motorized stage on a Zeiss Axiovert 35 inverted microscope (Carl Zeiss, Thornwood, NY), which was equipped with differential interference contrast optics. The temperature of the microscope objective (Zeiss 63×, 1.4 NA, Plan Apochromat), which was in thermal contact with the sample cell via immersion oil, was maintained at 23 ± 0.5°C. For illumination, a Zeiss 0.63 NA long-working-distance condenser was coupled to a 75-W xenon lamp (Opti Quip, Highland Mills, NY) via an optical fiber scrambler (Technical Video, Woods Hole, MA); critical illumination was used. A UV filter was placed in front of the xenon lamp to avoid photodamage to gramicidin. Video images were obtained with a Hamamatsu Newvicon video camera (Hamamatsu Corporation, Bridgewater, NJ) and recorded in S-VHS format.

The sample cell was filled with 400 μl of a solution consisting of 300 mM glucose and HCl (pH 1) and left open to the air. Evaporation had a negligible effect on membrane tension during the course of measurements on a single vesicle ($\lesssim$1 h) because the change in vesicle radius was less than 5% (see Eq. 1). A strip of 25-μm-thick tantalum foil (Goodfellow, Berwyn, PA) was placed in the cell to provide a support for bending the pipette into the focal plane of the microscope (Fig. 2 *A*). Approximately 0.5 μl of the vesicle solution (see above) was deposited in the cell.

The vesicles sediment because the sucrose solution in their interior is more dense than the glucose bath solution. In addition, the difference in index of refraction between the two solutions improves the optical contrast of the vesicles. The diameters of vesicles used in the experiment were in the range of 20–50 μm. Once a vesicle was aspirated, the stage was moved away from the field of vesicles so that the pipette tip was near the tantalum strip, and the pipette was lowered onto the strip until its tip was in the focal plane of the microscope.

Micropipettes were pulled from borosilicate capillaries (1-mm outer diameter, 0.75-mm inner diameter) (World Precision Instruments, Sarasota, FL) with a programmable puller (Sutter Instrument Company, Novato, CA) and cut and fire polished on a homemade forge. The typical tip diameter of micropipettes was 2 μm. (Micropipettes were measured after the experiments by visualizing in immersion oil.) Micropipettes were filled with the glucose/HCl solution, inserted in a holder containing a pressure port and AgCl electrode (World Precision Instruments), and attached to the headstage of an Axopatch 1A patch-clamp amplifier (Axon Instruments, Foster City, CA). HCl, which provided a source of ions for current flow, was chosen because of the relatively high conductivity of gramicidin channels to protons compared with other cations.

The aspiration pressure was controlled with a 60-cm^3 syringe and monitored with an MKS 223B capacitance manometer (MKS Instruments, Andover, MA). Typical pressures were in the range of 0–0.1 Pa. Membrane tension σ was computed from the formula (Kwok and Evans, 1981)

$$\sigma = \frac{PR_p}{2(1 - R_p/R_v)} \quad (1)$$

where P is the applied suction pressure, R_p is the inner radius of the pipette, and R_v is the radius of the portion of the vesicle outside of the pipette (Fig. 2 *B*). Video images were analyzed with the program NIH (National Institutes of Health, Bethesda, MD).

The sample cell contained an AgCl-coated silver wire (~4 cm), which was attached to the Axopatch headstage. Current recordings were made at holding potentials (V_h) of either 25 or 100 mV. The signal was low-pass filtered at 20, 100, or 200 Hz (−3-dB cutoff frequency). There was an electrical leak due to the aqueous layer between the vesicle and pipette wall, which corresponded to resistances in the range 50–130 MΩ for vesicle intrusions of 10–50 μm (Fig. 3). Leak subtraction was used to keep the amplified output voltage signal within the range ±10 V. The pressure, total current, and leak-subtracted current were all recorded on a Mac IIfx (Apple Computer, Cupertino, CA) equipped with a NIDAQ NB-MIO-16XH-18 analog-to-digital converter (National Instruments, Austin, TX) and running LabView (National Instruments); the sampling rate was 100 Hz (aliasing was not a problem, even at the higher filter frequencies).

Data analysis

To determine the gramicidin dimer lifetime, we used vesicles with a relatively low gramicidin/lipid ratio (GgA/lipid = 6×10^{-7}), so that the formation of individual dimers (single-channel events) could be easily resolved. Current records were visualized using our own software, and single-channel events were identified manually. Events that were ambiguous, either because there was more than one conducting channel, or because the single-channel current transitions could not be clearly resolved, were discarded.

The survival probability, $P(t)$, is the probability that a gramicidin dimer that forms at time $t = 0$ has not dissociated after time t. (The lifetime probability density function is equal to $-dP/dt$.) To calculate $P(t)$, all recorded dimerization events in a single vesicle at fixed tension were taken to open at $t = 0$. $P(t)$ was then computed from $P(t) = N(t)/N(0)$, where $N(t)$ is the number of dimers that remain after time t, and $N(0)$ is the initial number of dimers. Nonlinear fits to $P(t)$ were performed with Kaleidagraph (Synergy Software, Reading, PA).

To determine the dimer formation rate as a function of tension, we made measurements at different tensions in the same vesicle. GgA/lipid was in the range of $0.6–1.2 \times 10^{-6}$. The vesicles were first aspirated at a high pressure, and the current was recorded (usually for ~100 s). The pressure was then lowered in increments, with recordings at each pressure level. Attempts to move in increments from low to high pressure were unsuccessful because of vesicle breakdown, adhesion to the glass, or blebbing.

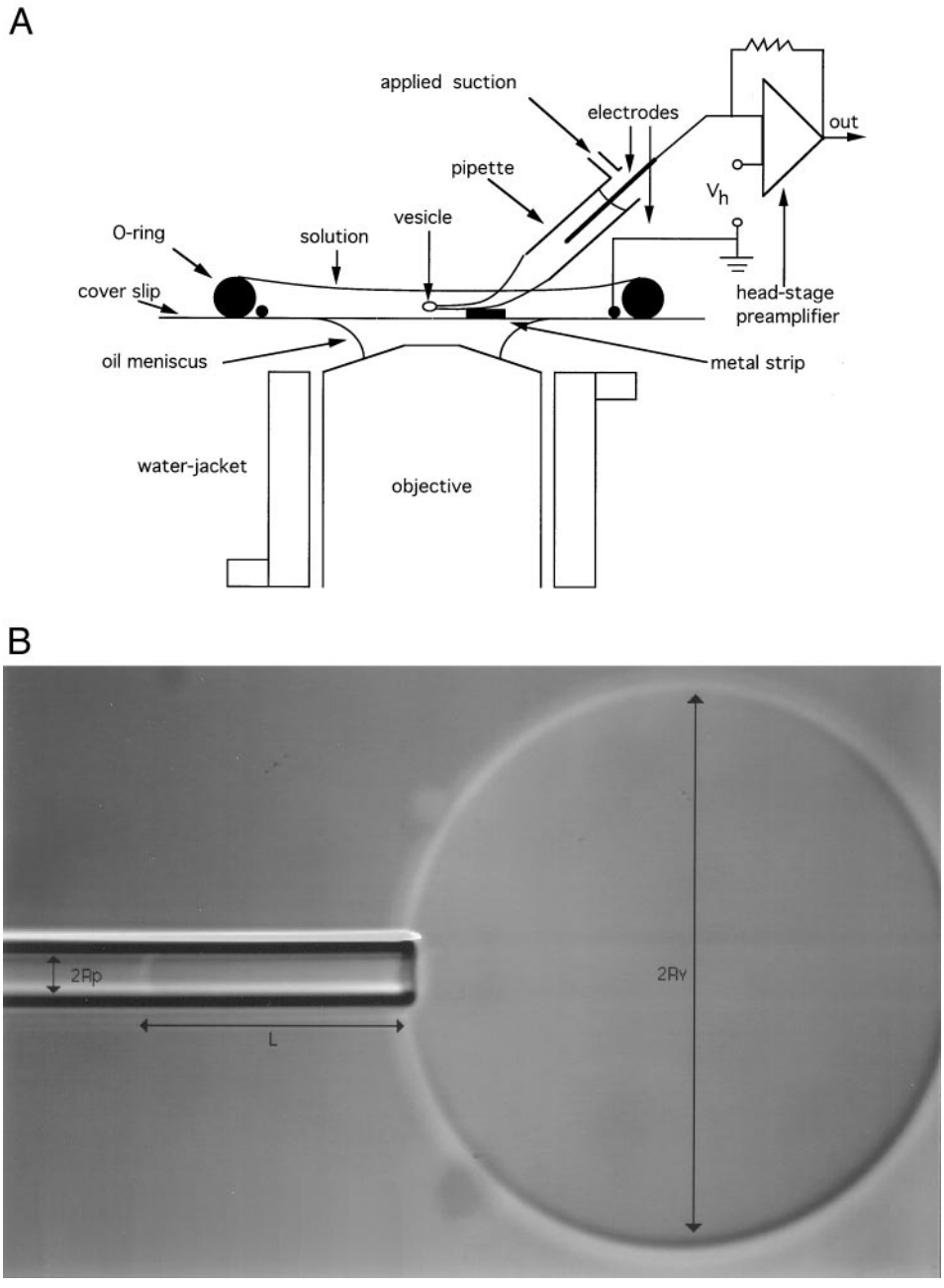

FIGURE 2 (*A*) The apparatus used for combined voltage clamp and pipette aspiration. See the text and Elbaum et al. (1996) and Fygenson et al. (1997) for details. (*B*) An aspirated vesicle in a typical field of view; R_p = 1.8 μm, R_v = 10 μm, and L = 20 μm.

To ensure that the results would not be biased by changes in the vesicle intrusion length L (Fig. 2 *B*), only results for which there was no more than 10% variation in the total current were analyzed. Formation rates were determined with our own software. Briefly, the time derivative of the current was calculated by locally fitting the current versus time to a line with a three- or nine-point fit (depending on the filter cutoff frequency). Points where the slope exceeded a threshold (which also depended on the filter cutoff) were counted as dimer formation events.

RESULTS

The combined pipette aspiration and single-channel recording technique described in this paper entails recording current flow through a micropipette containing an aspirated vesicle, as in Fig. 2 *B*. This leads to two important differences from conventional single-channel recording techniques, in which a single bilayer patch makes a high-resistance seal across a micropipette or hole in a teflon partition. First, for an aspirated vesicle, there is current flow between the glass and the vesicle intrusion. This leak resistance is in parallel with the membrane inside the pipette (inner membrane). Second, current continuity requires that current flowing through the inner membrane must also pass through the membrane outside the pipette (outer membrane), i.e., there is a resistance in series with the inner membrane. Below, we first characterize the leak resistance and give an example of single-channel recordings that are in parallel with the leak. We then show that the resistance of the outer membrane can be neglected.

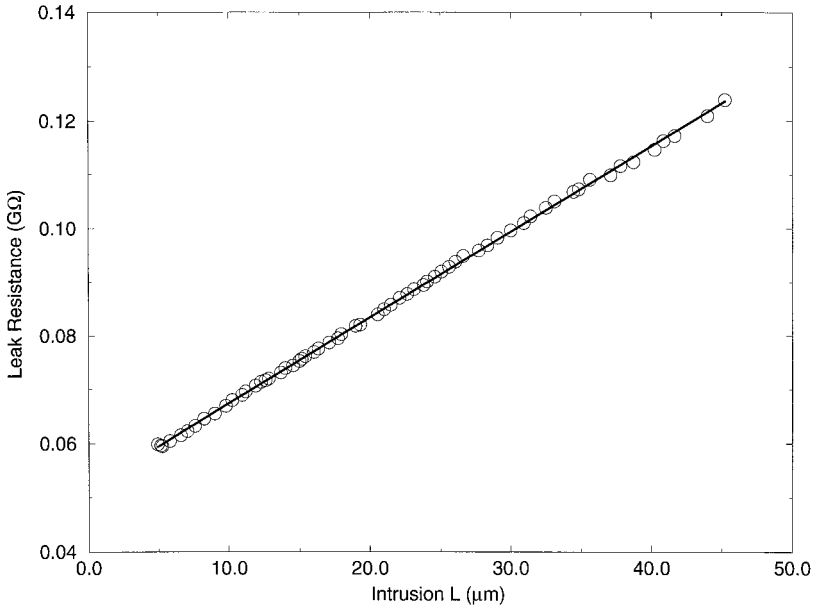

FIGURE 3 Pipette leak resistance versus intrusion length L. The linear fit has slope 2 MΩ/μm.

Vesicles aspirated at a fixed pressure usually drifted into the pipette continuously, but slowly, until they either blebbed or burst. In association with this drift, there was an increase in the leak resistance. Fig. 3 shows a plot of the pipette resistance as a function of intrusion length L for an aspirated vesicle. We attribute the electrical leak to current flow along the pipette within the aqueous layer between the membrane and the glass (Evans and Rawicz, 1990). Consistent with this interpretation, the pipette resistance is an approximately linear function of L, with a slope of $\sim$2 MΩ/μm. Taking the resistivity of 0.1 M HCl to be 30 Ω cm (Robinson and Stokes, 1968), this corresponds to an aqueous layer of thickness 25 nm.

For our measurements, this parallel leak resistance is unavoidable because for the membrane tension to be given by Eq. 1 (which is the reason for using pipette aspiration), there cannot be complete adhesion between the membrane and the glass. Even for intrusions as large as $L = 50$ μm, the pipette resistance was much smaller than the $\sim$10-GΩ resistance of a gramicidin channel (Fig. 3). Nevertheless, for $L > \sim 10$ μm, the leak was sufficiently quiet that single channels were easily resolved.

Fig. 4 *A* shows an example of channel recordings in parallel with the leak current. There is a pronounced modulation in the open-channel current. At least part of this modulation is due to diffusion of the gramicidin dimer within the membrane along the length of the pipette. Because the leak current creates a potential gradient running down the pipette, the open-channel current varies as the channel diffuses in this gradient. The variation in channel current makes lifetime measurements difficult, particularly for a long-lived channel such as VgA (lifetime $\approx$ 10 s), because conducting channels can diffuse into and out of the pipette. We therefore used the glycine-substituted variant [gly^1]gramicidin A (GgA), which has a shorter lifetime ($< \sim 1$ s) (Durkin et al., 1990; Mattice et al., 1995) for kinetic measurements.

Channels in the outer membrane do not interfere with our measurements because the outer membrane resistance is much less than the 10-GΩ resistance of a single channel. To show this, we take advantage of the fact that occasionally gigaseals formed with the outer membrane still intact, i.e., the leak resistance jumped to over 100 GΩ, presumably because of the membrane inside the pipette adhering to the glass. With gigaseals, we obtained single-channel recordings as in Fig. 4 *B*. Despite the improvement in signal-to-noise, records with gigaseals were not used for analysis because the tension of the membrane could not be determined (Eq. 1 no longer applies). Gigaseals, however, allow us to address the issue of membrane resistance.

As is evident from the current recordings in Fig. 4 *B*, there was, on average, less than one channel open in the vesicle membrane. Let us assume that the lipid bilayer has negligible conductivity. In this case, the formation of a gramicidin dimer inside the pipette would result in current transitions as in Fig. 4 *B* only if there were already a dimer present in the outer membrane. If a third channel then opened, in either the inner or outer membrane, the corresponding current transition would be a factor of one-third smaller than the first transition. However, the current transitions do not show this variation in height (Fig. 4 *B*). Furthermore, if there were no dimer present in the outer membrane, the formation of a dimer in the inner membrane would result in a current jump that would decay to zero with a time constant $RC \approx 100$ ms, where $R \approx 10$ GΩ is the channel resistance and $C \approx 10$ pF is the capacitance of the outer membrane for a 10-μm-radius vesicle. We do not see such current jumps, however. We therefore neglect the

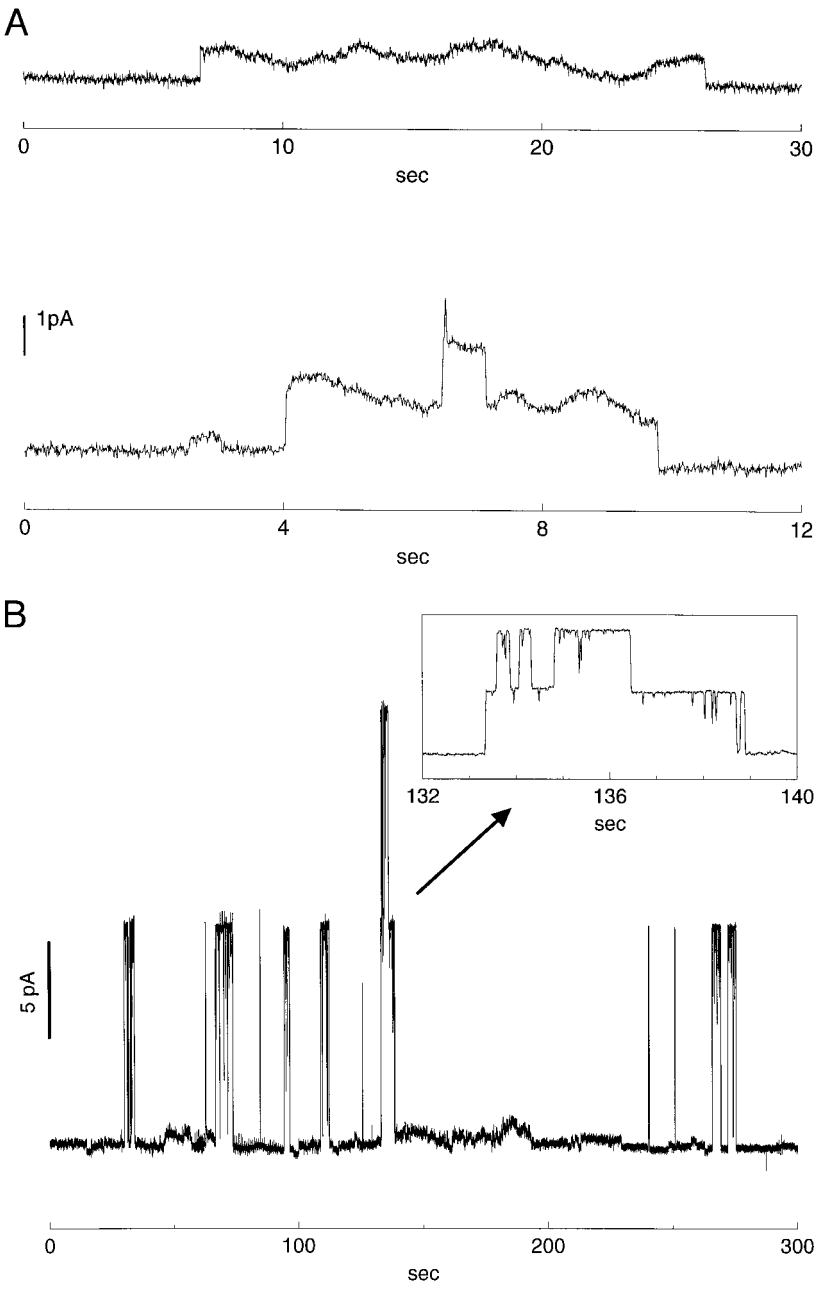

FIGURE 4 (*A*) Current recordings of VgA channels in the presence of a nonzero leak current. We attribute the modulation of the open-channel current to lateral diffusion of the channel in the potential gradient running down the length of the pipette. A current fluctuation of 0.1 pA corresponds to a displacement of 1 μm along the pipette. V_{hold} = 25 mV. (*B*) Example of single-channel recordings of VgA in the presence of a gigaseal, which forms when membrane sticks to the pipette along the entire circumference. The inset is an expanded view of events in which two channels were open simultaneously. V_{hold} = 100 mV.

resistance of the outer membrane and take the potential of the vesicle interior to be equal to the potential of the solution in the sample cell.

We have obtained a lower bound on the proton conductance of solvent-free DOPC bilayers from the results of one measurement in which a vesicle ruptured and part of the residual membrane formed a 20-GΩ seal several hundred microns up the pipette, where the pipette radius was 1.7 μm (data not shown). This implies a specific membrane conductance of $\leq$0.5 mS/cm^2, which gives a resistance of $\geq$200 MΩ for a 1000-μm^2 outer membrane. (Only a lower bound can be obtained, because we do not know the magnitude of the seal resistance.)

Lifetime

An example of the survival probability $P(t)$ for GgA dimers in a single vesicle at fixed tension is shown in Fig. 5 *A*. The results are well fit by a sum of two exponentials:

$$P(t) = [b \exp(-t/\tau_1) + (1 - b)\exp(-t/\tau_2)] \qquad (2)$$

with characteristic times τ_1 and τ_2 differing by an order of magnitude and $b \approx 1/2$, indicating approximately equal numbers of long-lived and short-lived events. The proliferation of short-lived events, which gave rise to the second time scale, did not appear in similar records for the longer lived VgA (lifetime $\approx$ 10 s) (results not shown). This

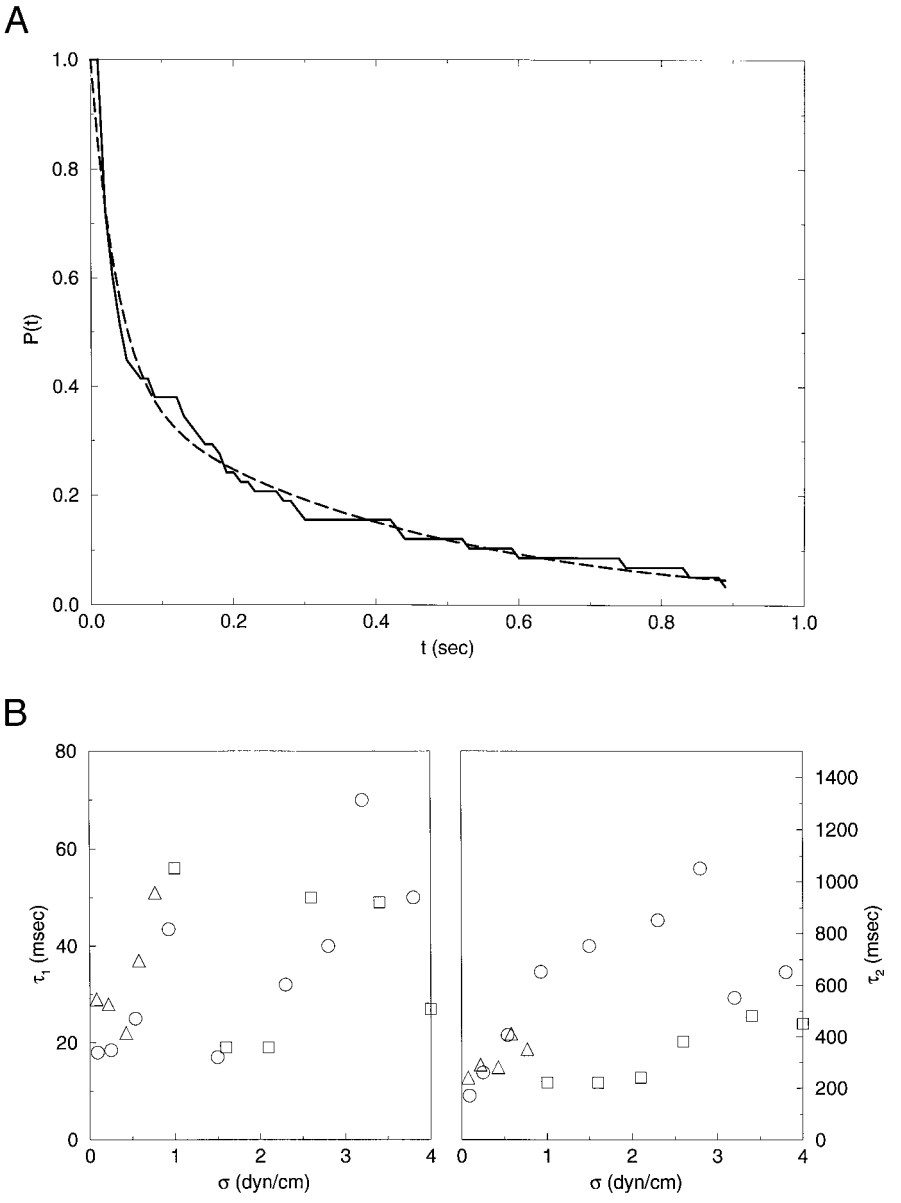

FIGURE 5 (*A*) Survival probability $P(t)$ of GgA from measurements in a single vesicle at fixed tension (0.58 dyn/cm), 58 events. The dashed curve is a two-exponential fit (Eq. 2) with $\tau_1 = 38$ ms, $\tau_2 = 430$ ms, $b = 0.61$. (*B*) Lifetimes τ_1 and τ_2, derived from two-exponential fits, versus membrane tension σ. The three different symbols correspond to measurements in three different vesicles.

suggests that the short time scale is a characteristic of GgA and not due to experimental artifacts, such as membrane flicker against the glass. Subsequent single-channel recordings of GgA in solvent-depleted DOPC-hexadecane bilayers, using a modified tip-dip method (Hanke et al., 1983; Sawyer et al., 1990), also showed two time scales in 0.1 M HCl, but not in CsCl or NaCl (C. Nielsen and O. S. Andersen, unpublished results). We do not understand the basis for this difference, but note that the presence of two time scales appears to be a general property of GgA in thin bilayers in 0.1 M HCl.

The results for the two lifetimes as a function of tension are shown in Fig. 5 *B*. τ_2 exhibits a trend toward increasing lifetime with tension. The trend in τ_1 is less clear. A number of factors contribute to the scatter in our results. First, it is more difficult to extract the lifetime of individual dimers at higher tension because the channel formation rate also increases with tension (see below). Second, the vesicles do not survive as long at high tension, making it difficult to obtain a large number of events. Typical numbers of events used to determine lifetimes ranged from 517 to 30, with a median of 56.

Formation rate

The dimer formation rate, the number of dimers that form per unit of time, depends on the number of gramicidin monomers and therefore is sensitive to the membrane area inside the pipette as well as fluctuations in gramicidin concentration from vesicle to vesicle. We therefore measured formation rates (for GgA) at different tensions in the same vesicle, where we only kept points for which the intrusion length L (as measured by the leak current) did not

vary by more than 10%. A large range of tensions could be probed by incrementally lowering the tension, which worked against the tendency of intrusions to drift further into the pipette. An example of data from such a measurement is shown in Fig. 6 *A*, which plots the number of dimers formed per second, f, as a function of tension σ. The curve is a quadratic fit to the data: $\ln f = C_0 + C_1\sigma + C_2\sigma^2$. Based on 12 such plots (12 different vesicles), the average values for C_1 and C_2 are $\bar{C}_1 = 0.9$ cm/dyn and $\bar{C}_2 = -0.12$ cm^2/dyn^2 (for GgA). The coefficient C_0 is the logarithm of the formation rate at zero tension and is therefore sensitive to the density of gramicidin molecules. Plots of C_1 versus C_0 and C_2 versus C_0 show no obvious correlations (results not shown). This suggests that the observed saturation in the formation rate at high tension is not a result of depleting the population of gramicidin monomers. Fig. 6 *B* shows a combined plot of all 12 measurements in which each data set has been shifted so as to obtain the best quadratic fit for the combined sets (shown in the *solid curve*). The coefficients of the quadratic fit are $C_1 = 0.7$ cm/dyn and $C_2 = -0.09$ cm^2/dyn^2. For the average over individual fits and from the combined quadratic fit of the aggregate data, we find that the formation rate increases by roughly a factor of 5 as tension ranges from 0 to 4 dyn/cm.

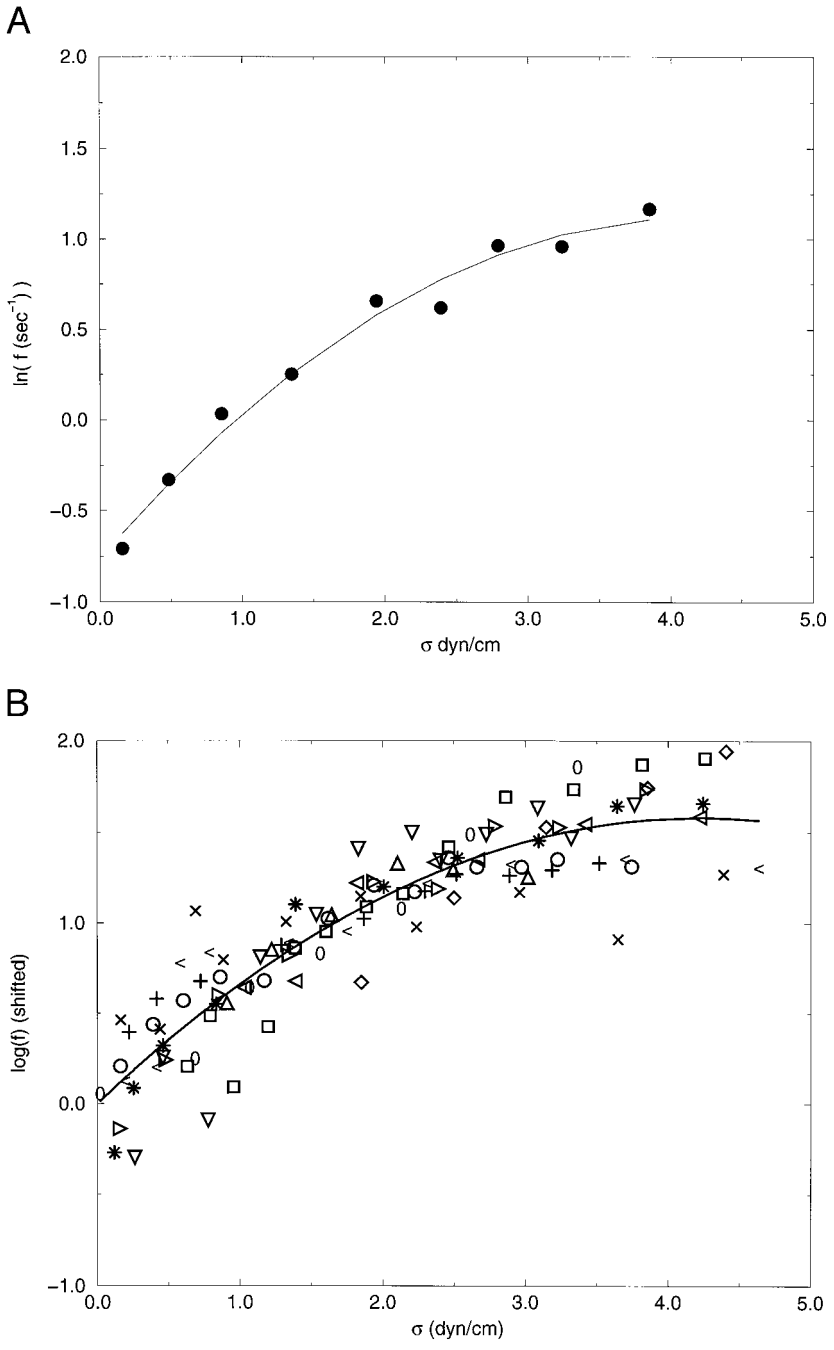

FIGURE 6 (*A*) Plot of the logarithm of the formation rate f of GgA versus tension σ for a single vesicle. The curve is a quadratic fit: $\log(f) = -0.8 + 0.9(\text{cm/dyn})\sigma - 0.1(\text{cm}^2/\text{dyn}^2)\sigma^2$. (*B*) Combined plot of 12 different measurements of formation rate versus tension (*represented by different symbols*). Each curve has been shifted by a constant to obtain the best quadratic fit for the combined data (shown in the *solid curve*). The solid curve is given by $\ln f = 0.7(\text{cm/dyn})\sigma - 0.08(\text{cm}^2/\text{dyn}^2)\sigma^2$.

DISCUSSION

For tension to affect channel formation there must be an associated change in membrane area. For example, alamethicin, a different channel-forming peptide, creates pores of varying size, with larger pores favored at higher tensions (Opsahl and Webb, 1994). For gramicidin, on the other hand, the area occupied by the peptide is approximately the same for monomers and dimers. Instead, the tension dependence stems from the thickness mismatch between dimer and membrane. An increase in tension increases the area per lipid and therefore decreases the membrane thickness. This, in turn, changes the elastic stress on the gramicidin dimer.

The hydrophobic thickness of a DOPC bilayer is 27 ± 1 Å (Lewis and Engelman, 1983). Although the corresponding hydrophobic thickness of a gramicidin dimer has not been determined, it is generally believed to be less than the full 26-Å dimer length (Urry, 1972) and has been estimated to be on the order of ~22 Å (Elliott et al., 1983). For a tension σ, the work performed in forming the dimer, as a result of tension acting directly on gramicidin, will be approximately $\sigma\pi r_o(d - l)\sin\theta$ (Elliott et al., 1983), where $r_o = 10$ Å and $l = 22$ Å are the gramicidin dimer radius and thickness, d is the membrane thickness, and θ is the angle depicted in Fig. 7 *A*. Because $\theta \ll 1$, even a tension of 4 dyn/cm will result in mechanical work that is much less than the thermal energy k_BT. In addition, for this work to result in an increase in dimer formation rate and lifetime, the angle θ would have to be negative. It is therefore unlikely that the direct action of tension on gramicidin significantly perturbs the dimerization kinetics.

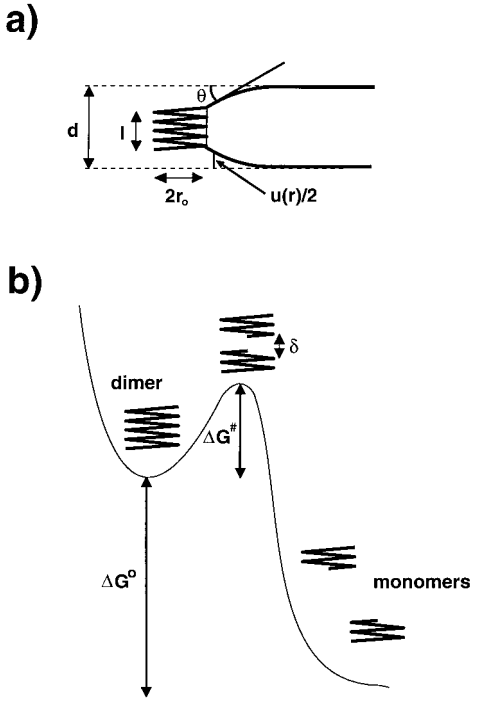

FIGURE 7 (*A*) The membrane has an unperturbed thickness d. $u(r)$ is the deviation in membrane thickness from d, r_o and l are the gramicidin dimer radius and thickness, and θ is the contact angle between the membrane and dimer. (*B*) $\Delta G°$ is the free energy difference between dimer and monomers, and $\Delta G^{\#}$ is the activation barrier for dimer dissociation. At the peak of the activation barrier, the monomers are separated by a distance δ, which is roughly the range of the hydrogen bonds holding the dimer together. At the dilute concentrations of gramicidin used in our experiments, the dimer has a higher free energy compared with the monomers.

Tension, however, also acts by thinning the membrane. Because the bilayer is effectively "incompressible" with respect to volume changes (Evans and Hochmuth, 1978; Evans and Needham, 1987), an applied tension σ results in a change in bilayer thickness Δd:

$$\frac{\Delta d}{d_o} = -\frac{\sigma}{K_a} \tag{3}$$

where d_o is the bilayer thickness at zero tension and K_a is the area expansion modulus. For example, for typical values $K_a = 100$–200 dyn/cm, a change in tension of 4 dyn/cm thins the bilayer by 4–2%. The lipid acyl chains adjacent to gramicidin dimers are therefore compressed, and the relative free energy between dimer and monomers, as well as the activation barrier for dimer dissociation, will have components that depend on the membrane-gramicidin hydrophobic mismatch (Huang, 1986; Lundbæk and Andersen, 1994).

The kinetics of dimerization are described by

$$\frac{d\mathcal{N}_d}{dt} = k_+\mathcal{N}_m^2 - k_-\mathcal{N}_d$$
$$\mathcal{N} = \mathcal{N}_m + 2\mathcal{N}_d \tag{4}$$

where $\mathcal{N}$ is the total gramicidin concentration and $\mathcal{N}_m$ and $\mathcal{N}_d$ are the monomer and dimer concentrations, respectively. The rate constants are expected to take the usual form for an activated process:

$$k_+ = \nu_+\exp[-(\Delta G^o + \Delta G^{\#})/k_BT] \tag{5}$$

$$k_- = \nu_-\exp[-\Delta G^{\#}/k_BT] \tag{6}$$

where $\Delta G°$ is the free-energy difference between dimer and monomer and $\Delta G^{\#}$ is the activation energy for dimer dissociation (Fig. 7 *B*). In principle, the microscopic constants $\nu_{\pm}$ could depend on membrane tension; we expect such an effect to be small, however, and take them to be constant. The average dimer lifetime is equal to $1/k_-$, and the formation rate is given by $f = k_+\mathcal{N}_m^2$. Assuming that $\mathcal{N}_m$ is approximately constant (i.e., $\mathcal{N}_m \gg \mathcal{N}_d$),

$$\ln(f) = \text{constant} - \frac{\Delta G^o}{k_BT} - \frac{\Delta G^{\#}}{k_BT} \tag{7}$$

$\Delta G°$ and $\Delta G^{\#}$ both have components that depend on the elastic deformation of the membrane. Let $E(x)$ be the elastic energy of a membrane containing a gramicidin dimer of hydrophobic thickness x. Because the attractive potential giving rise to the gramicidin dimer is due to hydrogen bonds, the peak of the activation barrier for dimer dissoci-

ation corresponds to a small separation, δ, between monomers ($\delta < \sim 1$ Å; Fig. 7 *B*), which could, for example, result from a rotation of the monomers relative to each other. We therefore take

$$\Delta G^{\#} = E(l - \delta) - E(l) + \Delta G_o^{\#} \tag{8}$$

$$\Delta G^{o} = E(l) + \Delta G_o^{o} \tag{9}$$

where $\Delta G_o^{\#}$ and $\Delta G_o{}^{\circ}$ denote terms that do not depend on the membrane elasticity (and therefore are independent of tension). From Eq. 8 it is apparent that the small size of δ implies that membrane tension will have a much weaker effect on channel lifetime than on formation rate, which is consistent with our observations (see also Lundbæk et al., 1997).

The modest increase in gramicidin dimer lifetime with tension that we observe is quite different from the strong decrease in lifetime with tension reported by Elliott et al. (1983). In their experiments, however, membranes at different tensions had different thicknesses (different lipid compositions) and may have also contained different concentrations of solvent. It therefore is likely, in light of our results, that factors other than tension, such as changes in membrane thickness and local composition, were responsible for the large variation in lifetimes they measured.

To calculate $E(l)$, we turn to a phenomenological model of bilayer deformation (Huang, 1986; Helfrich and Jakobsson, 1990; Dan et al, 1993, 1994; Ring, 1996; Nielsen et al., manuscript in preparation). If $u(r)$ denotes the perturbation of the bilayer thickness as a function of lateral position r (Fig. 7), then the elastic energy for this perturbation is taken to be

$$E = \frac{1}{2}\int \mathrm{d}^2 r \left[\frac{K_c}{4}(\nabla^2 u)^2 + \alpha(\nabla u)^2 + \frac{K_a}{d_o^2}u^2\right] \tag{10}$$

The constants K_c, K_a correspond to curvature and expansion moduli, and α to membrane tension. It is important to realize that these constants are microscopic quantities—they may not correspond exactly to macroscopic values measured experimentally. Nevertheless, it is reasonable to expect at least a rough correspondence. From scaling (as well as explicit calculation) α can be neglected, provided $\alpha \ll \sqrt{K_c K_a / d_o^2}$, which will be the case for reasonable values of α. For simplicity, we therefore take $\alpha = 0$. We assume that the gramicidin dimer (located at the origin) imposes the boundary conditions

$$u|_{r=r_o} = d - l \qquad \left.\frac{\partial u}{\partial r}\right|_{r=r_o} = s \qquad u|_{r=\infty} = 0 \tag{11}$$

where $s = -2\tan\theta$, and $d = d_o - d_o\sigma/K_a$ is the hydrophobic thickness of the unperturbed (but tense) membrane. Minimizing Eq. 10 with respect to $u(r)$ gives

$$E(l) = K_c\left[s^2 f_0(r_o/\lambda) + f_1(r_o/\lambda)s\frac{(d-l)}{r_o} + f_2(r_o/\lambda)\frac{(d-l)^2}{r_o^2}\right]$$

$$\lambda \equiv \left(\frac{d_o^2 K_c}{K_a}\right)^{1/4} \tag{12}$$

with f_0, f_1, f_2 dimensionless functions, which can be expressed in terms of Bessel functions (Nielsen et al., manuscript in preparation). The quadratic dependence of E on σ follows directly from the linear relation between d and σ and the fact that Eq. 12 is quadratic in $d - l$.

From Eqs. 9–12, we find that the logarithm of the formation rate will depend quadratically on tension: $\ln(f) = C_0 + C_1\sigma + C_2\sigma^2$. With reasonable values of the parameters, we find good agreement with the fitted values from experiment. For example, with $l = 22$ Å, $d_o = 27$ Å, $r_o = 10$ Å, $K_a = 120$ dyn/cm, $K_c = 5.6 \times 10^{-12}$ erg, $\delta = 1$ Å, and $s = -0.3$, we find that $C_1 = 0.7$ cm/dyn and $C_2 = -0.09$ cm^2/dyn^2, which are the values we obtained from the combined quadratic fit (see above).

CONCLUSION

By combining the single-channel recording and pipette aspiration techniques, we have measured gramicidin A dimerization kinetics as a function of tension in a single-component membrane. Both the gramicidin dimer lifetime and formation rate increase with tension, the latter increasing by a factor of 5 as tension ranges from 0 to 4 dyn/cm. This behavior can be understood by using a phenomenological model of membrane elasticity, in which tension thins the membrane and thereby changes the membrane-dimer mismatch in hydrophobic thickness. We find good agreement with the data for reasonable parameter values. Our results demonstrate in a simple system how membrane deformation can modulate protein function. By applying the techniques described here to the study of other membrane proteins under tension, it should be possible to further probe this elusive but important aspect of membrane biophysics.

We thank E. Moses, who participated in the early stages of this experiment; R. E. Koeppe, II, for providing us with samples of purified [Val^1]gramicidin A and [Gly^1]gramicidin A; and H. Davidowitz, B. Houchmandzadeh, and P. Kaplan for helpful discussions.

MG is a W. M. Keck Fellow. ONM received partial support from the Brazilian Agency CNPq. OSA and CN were supported by National Institutes of Health grant GM21342. CN was also supported by the Danish Natural Science Research Council, SNF grant 11-1219-1. AL received support from the Mathers Foundation.

REFERENCES

Abney, J. R., and J. C. Owicki. 1985. Theories of protein-lipid and protein-protein interactions in membranes. *In* Progress in Protein-Lipid Interactions. A. Watts and J. J. H. H. M. De Pont, editors. Elsevier, Amsterdam. 1–60.

Andersen, O. S. 1983. Ion movement through gramicidin A channels. Single-channel measurements at very high potentials. *Biophys. J.* 41: 119–133.

Andersen, O. S., G. Saberwal, D. V. Greathouse, and R. E. Koeppe, II. 1996. Gramicidin channels—a solvable membrane "protein" folding problem. *Indian J. Biochem. Biophys.* 33:331–342.

Bamberg, E., and P. Läuger. 1973. Channel formation kinetics of gramicidin A in lipid bilayer membranes. *J. Membr. Biol.* 11:177–194.

Bienvenüe, A., and J. S. Marie. 1994. Modulation of protein function by lipids. *Curr. Top. Membr.* 40:319–354.

Cifu, A. S., R. E. Koeppe, II, and O. S. Andersen. 1992. On the supramolecular structure of gramicidin channels. The elementary conducting unit is a dimer. *Biophys. J.* 61:189–203.

Dan, N., A. Berman, P. Pincus, and S. A. Safran. 1994. Membrane-induced interactions between inclusions. *J. Phys. II France.* 4:1713–1725.

Dan, N., P. Pincus, and S. A. Safran. 1993. Membrane-induced interactions between inclusions. *Langmuir.* 9:2768–2771.

Devaux, P. F., and M. Seigneuret. 1985. Specificity of lipid-protein interactions as determined by spectroscopic techniques. *Biochim. Biophys. Acta.* 822:63–125.

Durkin, J. T., R. E. Koeppe, II, and O. S. Andersen. 1990. Energetics of gramicidin hybrid channel formation as a test for structural equivalence. Side-chain substitutions in the native sequence. *J. Mol. Biol.* 211: 221–234.

Elbaum, M., D. K. Fygenson, and A. Libchaber. 1996. Buckling microtubules in vesicles. *Phys. Rev. Lett.* 76:4078–4081.

Elliott, J. R., D. Needham, J. P. Dilger, and D. A. Haydon. 1983. The effects of bilayer thickness and tension on gramicidin single-channel lifetime. *Biochim. Biophys. Acta.* 735:95–103.

Evans, E. A., and R. M. Hochmuth. 1978. Mechanochemical properties of membranes. *In* Current Topics in Membranes and Transport, Vol 10. F. Bronner and A. Kleinzeller, editors. Academic Press, New York. 1–64.

Evans, E. A., and D. Needham. 1987. Physical properties of surfactant bilayer membranes: thermal transitions, elasticity, rigidity, cohesion, and colloidal interactions. *J. Phys. Chem.* 91:4219–4228.

Evans, E. A., and W. Rawicz. 1990. Entropy-driven tension and bending elasticity in condensed-fluid membranes. *Phys. Rev. Lett.* 64: 2094–2097.

Fygenson, D. K., M. Elbaum, B. Shraiman, and A. Libchaber. 1997. Microtubules and vesicles under controlled tension. *Phys. Rev.* E55: 850–859.

Gennis, R. B. 1989. Biomembranes: Molecular Structure and Function. Springer Verlag, New York.

Goulian, M. 1996. Inclusions in membranes. *Curr. Opin. Colloid Interface Sci.* 1:358–361.

Hanke, W., C. Methfessel, H.-U. Wilmsen, E. Katz. G. Jung, and G. Boheim. 1983. Melittin and a chemically modified trichotoxin form alamethicin-type multi-state pores. *Biochim. Biophys. Acta.* 727: 108–114.

Helfrich, P., and E. Jakobsson. 1990. Calculation of deformation energies and conformations in lipid membranes containing gramicidin channels. *Biophys. J.* 57:1075–1084.

Huang, H. W. 1986. Deformation free energy of bilayer membrane and its effect on gramicidin channel lifetime. *Biophys. J.* 50:1061–1070.

Koeppe, R. E., II, and O. S. Andersen. 1996. Engineering the gramicidin channel. *Annu. Rev. Biophys. Biomol. Struct.* 25:231–258.

Kwok, R., and E. Evans. 1981. Thermoelasticity of large lecithin bilayer vesicles. *Biophys. J.* 35:637–652.

Lewis, B. A., and D. M. Engelman. 1983. Lipid bilayer thickness varies linearly with acyl chain length in fluid phosphatidylcholine vesicles. *J. Mol. Biol.* 166:211–217.

Lundbæk, J. A., and O. S. Andersen. 1994. Lysophospholipids modulate channel function by altering the mechanical properties of lipid bilayers. *J. Gen. Physiol.* 104:645–673.

Lundbæk, J. A., A. M. Maer, and O. S. Andersen. 1997. Lipid bilayer electrostatic energy, curvature stress, and assembly of gramicidin channels. *Biochemistry.* 36:5695–5701.

Mattice, G. L., R. E. Koeppe, II, L. L. Providence, and O. S. Andersen. 1995. Stabilizing effect of D-alanine[2] in gramicidin channels. *Biochemistry.* 34:6827–6837.

Mouritsen, O. G., and M. Bloom. 1993. Models of lipid-protein interactions in membranes. *Annu. Rev. Biophys. Biomol. Struct.* 22:145–171.

Needham, D., and E. Evans. 1988. Structure and mechanical properties of giant lipid (DMPC) vesicle bilayers from 20°C below to 10°C above the liquid crystal-crystalline phase transition at 24°C. *Biochemistry.* 27: 8261–8269.

O'Connell, A. M., R. E. Koeppe, II, and O. S. Andersen. 1990. Kinetics of gramicidin channel formation in lipid bilayers: transmembrane monomer association. *Science.* 250:1256–1259.

Opsahl, L. R., and W. W. Webb. 1994. Transduction of membrane tension by the ion channel alamethicin. *Biophys. J.* 66:71–74.

Reeves, J. P., and R. M. Dowben. 1969. Formation and properties of thin-walled phospholipid vesicles. *J. Cell Physiol.* 73:49–60.

Ring, A. 1996. Gramicidin channel-induced lipid membrane deformation energy: influence of chain length and boundary conditions. *Biochim. Biophys. Acta.* 1278:147–159.

Robinson, R. A., and R. H. Stokes. 1968. Electrolyte Solutions: The Measurement and Interpretation of Conductance, Chemical Potential, and Diffusion in Solutions of Simple Electrolytes. Butterworths, London.

Sackmann, E. 1983. Physical foundations of the molecular organization and dynamics of membranes. *In* Biophysics. W. Hoppe, W. Lohmann, H. Markl, and H. Ziegler, editors. Springer Verlag, New York. 425–457.

Sawyer, D. B., R. E. Koeppe, II, and O. S. Andersen. 1989. Induction of conductance heterogeneity in gramicidin channels. *Biochemistry.* 28: 6571–6583.

Sawyer, D. B., S. Oiki, and O. S. Andersen. 1990. Single channels formed by gramicidin A in "solvent-free" bilayers formed from surface monolayers using a tip-dip technique. *Biophys. J.* 57:100a.

Urry, D. W. 1972. Protein conformation in biomembranes: optical rotation and absorption of membrane suspensions. *Biochim. Biophys. Acta.* 265: 115–168.

Veatch, W. R., R. Mathies, M. Eisenberg, and L. Stryer. 1975. Simultaneous fluorescence and conductance studies of planar bilayer membranes containing a highly active and fluorescent analog of gramicidin A. *J. Mol. Biol.* 99:75–92.